

ARTICLE OPEN



Towards the technological maturity of membrane distillation: the MD module performance curve

Pablo López-Porfiri^{1,5}, Sebastián Ramos-Paredes^{2,5}, Patricio Núñez² and Patricia Gorgojo^{1,3,4}✉

Membrane distillation (MD) is constantly acknowledged in the research literature as a promising technology for the future of desalination, with an increasing number of studies reported year after year. However, real MD applications still lag behind with only a few pilot-plant tests worldwide. The lack of technology transfer from academia to industry is caused by important gaps between its fundamental basis and the process design. Herein, we explore critical disconnections by conducting coupled mass and heat transfer modeling and MD simulations; we use well-known MD mass and heat transfer equations to model and simulate flux over a typical MD membrane for different geometries, areas, and operational conditions in direct contact configuration. From the analysis of the results, we propose research guidelines and process development strategies, and construct an *MD module performance curve*. From this graph, permeate flow rate, thermal energy consumption and outlet temperatures can be determined for given feed inlet conditions (temperature and concentration). Comprehensive tools such as this MD module curve and good communication between membrane developers and process engineers are required to accelerate the process of bringing the MD technology from a still-emerging status to a maturity level.

npj Clean Water (2023)6:18; <https://doi.org/10.1038/s41545-023-00234-0>

INTRODUCTION

Water has been recognized by the United Nations (UN) as a connector to climate change and other sectors; correct management of water resources is essential to accomplish several of the UN sustainable development goals (SDG)¹. Seawater has been identified as a nonconventional hydric resource to increase freshwater supply within 100 km of the coastline, where 40% of the world's population dwells². The idea of desalinization was first introduced in the XVIII century, but it was not until the 1960s that it fully developed³. Current technologies in commercial desalinization plants are multi-effect distillation (MED)⁴, multi-stage flash (MSF)⁵, and reverse osmosis (RO)⁶, with growing interest in other membrane-based processes⁷. Worldwide, desalinization has experimented an exponential growth reaching an annual capacity of about 35 billion m³ within 15,900 operational plants⁸. The major shares of these plants are based on conventional technologies, with 7% of MED, 18% of MSF, and 69% of RO. Notwithstanding, current conventional technologies are known for their extensive pre-treatment requirements as well as high-energy consumption. This last factor is strongly associated with greenhouse gas emissions, which jeopardize sustainability. The production of a cubic meter of drinking water from seawater demands 2.6–8.5 kWh, which translates into emissions of 1.7–25 kg of CO₂⁹.

Membrane distillation (MD) is acknowledged as an alternative membrane-based approach that could potentially alleviate the aforementioned high CO₂ emissions in the desalination industry and allows efficient operation at high salt concentrations¹⁰. Early work on MD was reported in the late 60 s, yet it is still considered an emerging technology. Contrary to the electricity/pressure-driven RO, water permeation in MD is driven by a thermal process with minor electrical energy consumption. The electric energy required for RO is estimated at 2.5–7.0 kWh per m³ vs the 0.6–1.8

kWh per m³ needed for MD. The main difference lies in the high pressure (20–100 bar) that the RO pumps need to overcome the osmotic pressure and allow water to permeate through the membrane at a reasonable rate¹¹. It is worth noting that pre-treatments to avoid fouling in RO are more complex, thus more expensive, than simple candle filters or the addition of biodegradable antiscalants that have been reported for MD¹². 90–98% of the total energy requirement in MD is thermal energy¹³, but the low-temperature gradients (30–80 °C) needed to carry out desalinization by MD makes it possible to directly couple it with renewable sources of thermal energy such as solar collectors or waste heat^{14,15}.

However, its technological maturity is far from that of other well-established systems. Despite the relatively large number of research articles on MD, patent applications on equipment and MD processes or membrane development itself have remained relatively constant over the last decade¹⁶. The observed absence of invention wane or sustained growth delays technological transfer to industry. These barriers to large-scale implementation have been previously identified by other authors¹⁷.

This article aims to help researchers and engineers gear their work towards a more focused approach in the MD field to bring the technology to a higher technology readiness level (TRL); that is, above TRL 6: system demonstration and up to TLR 8: actual system completed and qualified¹⁸. A deep understanding of the MD process and new engineering design tools will aid in its scale-up implementation and will allow for more reliable project evaluation strategies. Herein, a more accurate approach for the scale-up procedure is presented, and a module performance curve is constructed for a typical MD membrane and a range of operational parameters.

¹Department of Chemical Engineering, Faculty of Science and Engineering, The University of Manchester, Manchester M13 9PL, UK. ²Departamento de Ingeniería Química y Ambiental, Universidad Técnica Federico Santa María, Avda. España, 1680 Valparaíso, Chile. ³Instituto de Nanociencia y Materiales de Aragón (INMA) CSIC-Universidad de Zaragoza, C/ Mariano Esquillor s/n, 50018 Zaragoza, Spain. ⁴Departamento de Ingeniería Química y Tecnologías del Medio Ambiente, Universidad de Zaragoza, C/ Pedro Cerbuna 12, 50009 Zaragoza, Spain. ⁵These authors contributed equally: Pablo López-Porfiri, Sebastián Ramos-Paredes. ✉email: p.gorgojo@manchester.ac.uk

RESULTS AND DISCUSSION

Accurate predictive models for new separation processes are needed to make operational predictions as reliable as those in mature techniques such as conventional tray distillation¹⁹. The roadmap of any technology development starts from its theoretical conceptualization and continues with the development of predictive models and equipment sizing procedures that feed into process design for techno-economic evaluations, as shown in Fig. 1 for MD. Unfortunately, communication between these technology development levels in MD often fails. The fundamental basis usually supports the observed experimental results but is rarely used for predicting them. Despite the deep understanding of the phenomena at a micro-level and the exhaustive experimental efforts made at a macro one, techno-economic evaluation studies are carried out by simple extrapolation of the results from a single MD module without considering the effect of the interstage variations on its performance. These approaches are clearly an obstacle to overcoming the MD developmental bottlenecks. Therefore, to accomplish its technological maturity, MD needs to advance in two essential pillars: (i)

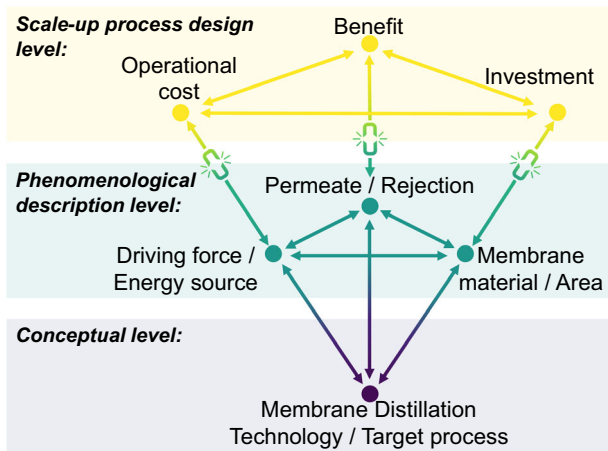


Fig. 1 Technology development levels in membrane distillation. Bottom, theoretical MD technology conceptualization; middle, process phenomenological description and predictive models; top, equipment sizing and process design for techno-economic evaluations.

research on fundamental phenomena description, enhanced membrane materials, and operational improvements; (ii) empirical demonstration of the process feasibility in real applications. A large number of reports on the use of novel materials for membrane fabrication can be found in the literature; with the discovery of graphene, there has been a growing interest in the use of carbon nanomaterials for MD applications^{20,21}. Well-known membrane issues such as scaling or fouling also affect MD, and different mitigation strategies, including anti-fouling materials and module cleaning techniques have been reported^{12,22}. A more specific problem for MD is pore wetting, which reduces separation capacity, and must be prevented²³.

Several comprehensive reviews can be found on MD at a theoretical level^{10,24}. Transmembrane permeation in MD is driven by the saturation pressure difference on the hot and cold sides as a consequence of the temperature gradient, as shown in Fig. 2. Yet, the underlying coupled phenomena is a complex set of mass and heat processes. For a simple direct contact (DCMD) configuration, mass transfer is controlled by both Knudsen (D_{Kn}) and molecular (D_{mol}) diffusion, whereas heat transfer takes place by convective (Q_h), conductive (Q_k), and evaporative (Q_A) flow mechanisms. The process becomes even more intricate for other most promising thermal-efficient or flux-enhanced configurations such as vacuum air gap (VAGMD)²⁵; the diffusion of water in the air (D_{w-air}), the convective heat in the gap zone, the vapor condensation effect (Q_{cond}) and the heat transfer in the condenser plate have to be also considered. Moreover, regardless of the configuration, MD is a coupled heat and mass transfer phenomenon, where the water permeation affects the driving force, i.e., the temperature gradient, on which the vapor flux depends in a feedback loop. The literature gives in-depth descriptions and correlations for the mass and heat transfer covering different MD configurations and geometries²⁶. However, when interpreting the obtained data, researchers usually split the mass-heat transfer phenomenon and discuss its effect separately. Such simplification has led to a misconception of the fundamental basis and errors in the scale-up procedures, thus limiting the impact of the studies on MD development.

Ongoing MD development efforts

It is not surprising that to date, there are two orders of magnitude more scientific MD publications, on both experimental and modeling, than MD pilot plants testing with a TRL equal to or

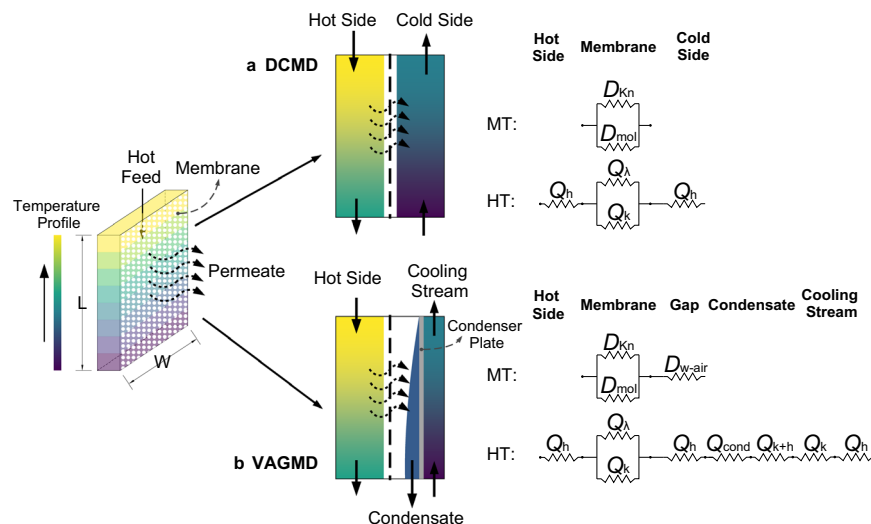


Fig. 2 Main membrane distillation configurations schemes. **a** Direct Contact Membrane distillation (DCMD); **b** Vacuum Airgap Membrane distillation (VAGMD). L: length, W: width. Mass transfer (MT) and heat transfer (HT) resistances represented as the diffusional regime (D_i) and heat mechanisms (Q_i), respectively.

above 8²⁷. The European Union HORIZON research and innovation funding program recently called for MD projects with a total budget of more than MM €400. Among the target activities to be covered by this Innovation Action (IA) are scale-up, solar energy integration, and sustainable membrane materials. The MD market offers several MD module vendors, yet very few major commercialization attempts are observed^{28,29}. South Korea has stated seawater desalination as a top priority R&D project, with a special focus on the RO brine treatment, achieving a hybrid MD-RO pilot plant with a capacity of 400 m³ per day under the Global MVP program³⁰. Other full-scale MD systems, 50–100 m³ per day, can be found in Singapore, Qatar, Maldives, and United Arab Emirates³¹.

Great research efforts have been made into overcoming one of the main MD limitations, i.e., membrane lifespan³². Pore wetting, scaling, and fouling are among the primary causes of membrane performance drop over time. Pore-wetting resistance has been improved by developing superhydrophobic membranes that optimize the pore structure and by new materials with omniphobic properties^{33,34}. Reduction of solute scaling or fouling has been achieved by coupling superhydrophobic materials with effective operational approaches, such as cleaning by gas purging³⁵. However, there is a trade-off between the aforementioned strategies, where improving one feature brings in another issue, hindering the development of an all-purpose membrane. Notably, the Janus membrane, a “two-faced” membrane with different natures, has been shown to be capable to show both fouling and wetting resistance³⁶. The high thermal energy requirement is another MD bottleneck to be overcome. In this aspect, efficient renewable energy linkage, development of new module configurations, and energy integration designs are the key research tasks.

Recent pilot plant projects and MD innovations have been developed aiming at filling the gaps and limitations in the technology. Multi-stage MD proposals have been studied to increase permeate production by improving energy recovery and increasing the total membrane area^{37,38}. Companies venturing into MD module manufacturing point out the advances made in new materials for membranes and new alternatives of MD configurations, mostly from air gap (AGMD) and vacuum

(VMD)^{27,39}. Performance evaluation of a scale-up DCMD system showed the temperature losses are greater and the permeate flows lower at the large scale than the small scale⁴⁰. The use of the residual thermal energy was identified as the most promising heat source for MD by a technical-economic study for AGMD and water gap (WGMD) seawater desalination at different scales of 10, 100, and 1000 m³ per day⁴¹. Exploiting the advantages of the different technologies in hybrid systems has also been recognized as the optimal path to reach a commercial and sustainable desalination process^{42,43}. However, a full behavior understanding of the stand-alone technologies is needed to accomplish the integration into existing plants. Moreover, standardized performance measurement and reporting are required to allow for a straightforward comparison. The same approach has been suggested for the energy consumption comparison of different desalination methods⁴⁴. The technology transfer from the laboratory to the industry can be significantly improved with the development of comprehensive coupled approaches to allow for feasible technology scale-up.

Understanding the MD modeling and module sizing

Unlike MD, mature technologies such as RO have well-established guidelines and software on plant design, process control, and engineering developments, broadly available in the literature⁴⁵. Membrane performance in MD can be obtained experimentally or predicted by theoretical modeling. However, reported experimental results in the literature normally lack some of the required data to do a proper scale-up module design; publications typically contain a brief description of the equipment, primary laboratory conditions, e.g., hot and cold side flowrates, reservoirs temperature, the membrane’s physical characteristics, and the average transmembrane water flux (kg m⁻² h⁻¹ or L m⁻² h⁻¹, LMH, units). Experimental error is another major issue regarding MD data reporting. Researchers often do not report the complete result uncertainties. Moreover, no mass or heat balances are performed to validate experimental measurements. Scaling-up processes require specific module dimensions and geometry inputs, as well as boundary conditions, e.g., stream flow rate, velocity, and inlet/

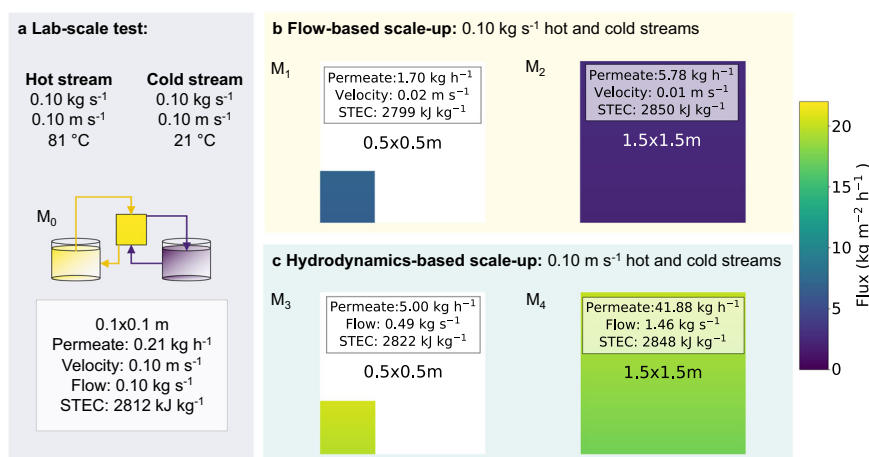


Fig. 3 Examples of the flow-based and hydrodynamics-based scale-up approaches. DCMD permeate flux, kg m⁻² h⁻¹, simulations over the membrane surface computed using a coupled mass and heat transfer phenomena model developed in this work. **a** Lab-scale membrane test (M_0) under defined conditions and an effective area of 0.01 m²; **b** scaled-up MD modules replicating the laboratory flow conditions of 0.10 kg s⁻¹; **c** scaled-up MD modules replicating the laboratory hydrodynamics conditions based on the flow velocity of 0.10 m s⁻¹. The Membrane performance, the total permeate water, is obtained from the flux integration over the membrane area differential. Hot and cold side flow ratios of 1:1 and inlet temperatures ($T_{\text{Hot}} = 81^\circ\text{C}$ and $T_{\text{Cold}} = 21^\circ\text{C}$) were maintained as constants for all simulations. The membrane material characteristics are PVDF; porosity: 75%; pore size of 0.45 μm ; and thickness: 140 μm . Salt content was not considered in any of the streams. The flow-based modules (M_1 and M_2) showed no permeate increment proportional to the area growth, contrary to the hydrodynamic-based modules (M_3 and M_4). No increment is observed for the specific thermal energy consumption per permeate unit (STEC), kJ kg⁻¹, which directly depends on the permeate rate over the membrane area.

outlet temperatures. These last parameters are imperative to corroborate the system mass and energy balance.

In this work, we demonstrate how an MD module performance can be predicted by using already-known MD mass and heat transfer phenomenology/equations to model and simulate flux over the entire membrane surface for different geometries, areas, and operational conditions for a typically reported MD membrane operating in direct contact mode^{46,47}. Membrane morphology (i.e., pore size, porosity, and thickness), operational conditions, permeate productivity, transmembrane heat efficiencies, and outlet temperatures have been investigated by coupled heat and mass models. Multistage scale-up simulations have been also performed. The model and simulation procedure are described in the section Methods, and detailed results are available in the Supplementary Information.

It is worth noting that pilot plant design based only on trial and error is economically unfeasible, and often relies on lab-scale data. At this scale, small areas of membrane samples are tested and are

often expected to describe the overall performance of large MD modules. The scaling-up process using the reported data from lab-scale experiments is often incorrect, as these data do not meet all the requirements to be properly introduced in the model. An example of this situation was simulated, and the results are displayed in Fig. 3.

For a membrane area of 0.01 m² (dimensions typically used at lab-scale), membrane M_0 in Fig. 3a, the flux decrease along the porous film is very small due to small changes in the thermal gradient, and thus an average flux is typically considered representative of the overall membrane performance. However, for large-scale modules (0.25–2.25 m²), where there are significant changes in the thermal gradient, fluxes are not constant, which leads to erroneous permeate values. M_1 and M_2 in Fig. 3b represent two membranes with areas of 0.25 m² (M_1) and 2.25 m² (M_2) that have been modeled using the reported small-scale (Fig. 3a) flowrates and temperatures, referred to as the flow-based approach. Under a more realistic approach, the so-called

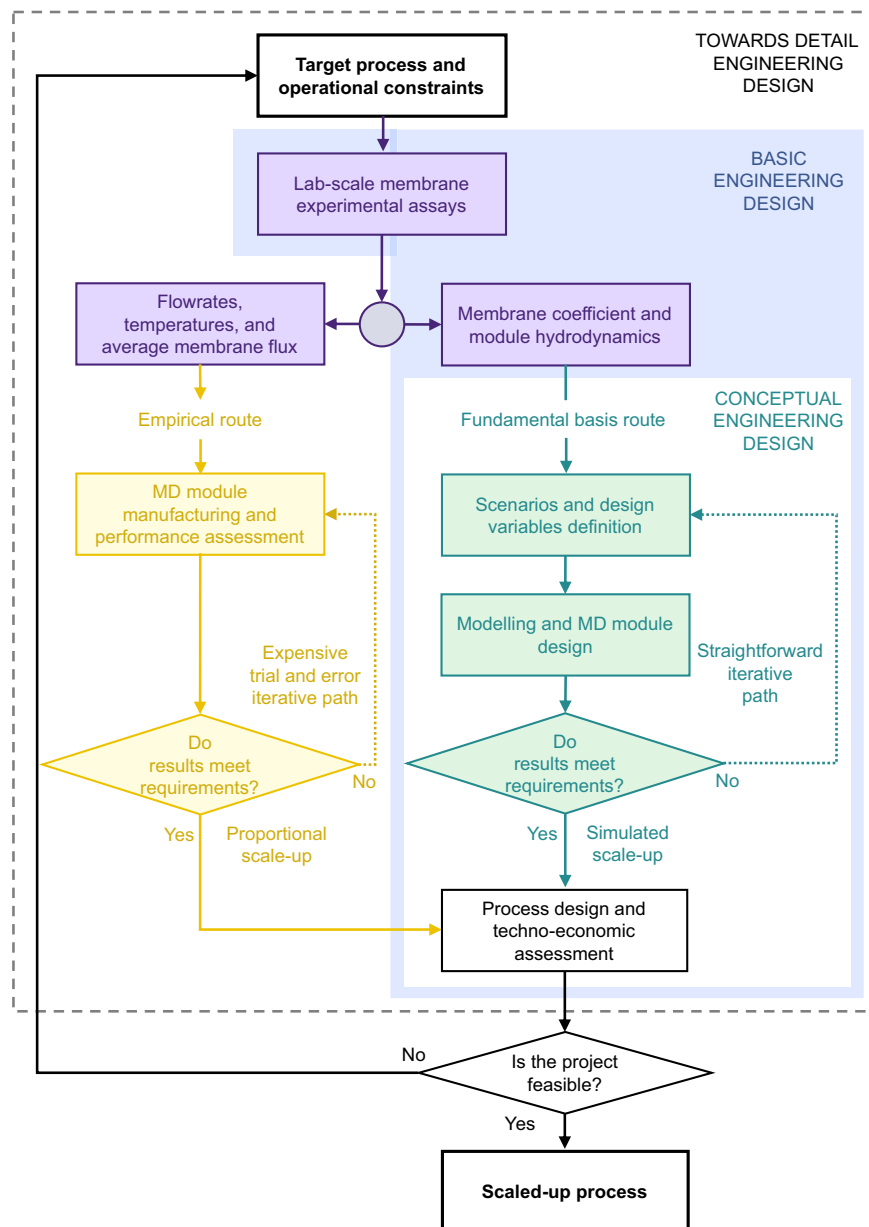


Fig. 4 Project development strategies for membrane distillation. In purple, the experimental MD assessments; in yellow, the empirical development route; in green, the fundamental basis development route.

hydrodynamics-based approach, the scale-up of the same membrane area and geometry of the above examples results in the M_3 and M_4 membranes in Fig. 3c. The results for M_3 and M_4 show big differences in water permeation, as compared to those predicted without considering thermal effects, thus it is key to replicate the small-scale hydrodynamics (stream velocities) and system operational conditions that determine the mass and heat transfers. It is demonstrated that transmembrane flux is a position-dependent parameter and thus, the membrane geometry should be optimized in any large-scale design approach.

The average flux, in consequence, is not the ideal membrane performance indicator. The predicted performance of the membrane module using both the flow-based (M_1 & M_2) and hydrodynamics-based (M_3 & M_4) models differ from the expected performance, i.e., proportional increments with the area. For the flow-based approach, larger areas lead to greater deviation (lower permeate increase) mainly due to the lower flowrates. On the

other hand, the hydrodynamics-based scaled-up membrane sheets exhibit a closer proportional permeate increment, but it is still not a linear function. This highlights the need for a thorough understanding of the fundamental basis in the MD modeling stage as well as to provide crucial experimental information to replicate the small-scale results into pilot-scale tests. It would be also recommended to address the experimental design considering the large-scale application. Some parameters can be optimized to increase the water permeation at a small-scale but are unviable at a larger scale. For instance, high stream velocities give a significant mass transfer improvement but can make the system unstable due to increasing equipment vibrations or compromise the membrane integrity. On the other hand, no increments of the specific thermal energy consumption, STEC (kJ kg^{-1}), are observed for all the above examples. Note that the reported STECs have been normalized by the permeate through the membrane sheet to allow for a proper comparison between

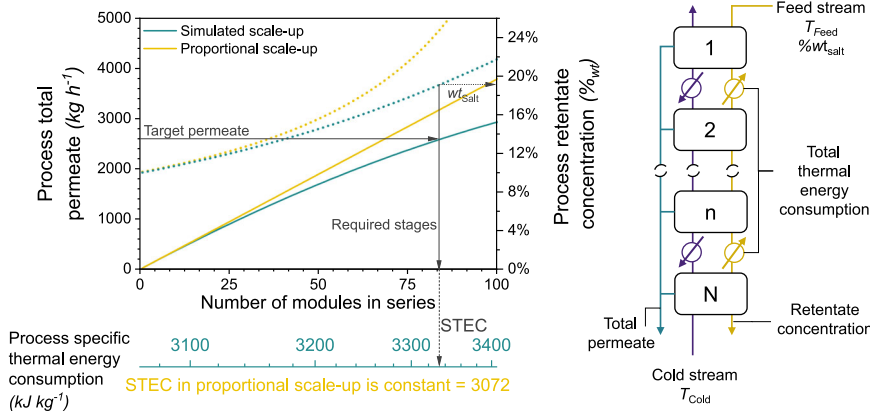


Fig. 5 Comparison of the predicted performance of a multi-stage MD process design of N modules in series. Given a target total permeate production (solid lines read to the left) the required number of modules in series, final brine concentration (segmented lines read to the right), and specific thermal energy consumption, STEC, (at the bottom axis of the chart) is obtained. In yellow, following the proportional strategy based on N times the MD module with empirical permeate = 38.0 kg h^{-1} and constant thermal energy consumption = 3072 kJ kg^{-1} ; and in green, by a process simulation algorithm. Membrane M_4 from Fig. 3c was used to simulate the multi-stage process following both approaches.

Table 1. Phenomenological descriptions of the DCMD coupled mass and heat transfer used in this work.

DCMD module scheme	Mass transfer	List of variables
	Permeate flux $J = C_m \cdot (P_H^* \cdot a_w - P_C^*)$	ΔH^{vap} Water vaporization enthalpy (kJ kg^{-1}) A Area (m^2) a_w Water activity (mol mol^{-1}) C_m Membrane coefficient ($\text{kg m}^{-2} \text{ Pa}^{-1} \text{ s}^{-1}$) C_p Heat capacity (kJ kg^{-1}) d_p Pore diameter (m) D Vapor in air diffusivity ($\text{m}^2 \text{ s}^{-1}$) F Stream flow (kg s^{-1}) h Convective coefficient ($\text{kW m}^{-2} \text{ K}^{-1}$) J Permeate flux ($\text{kg m}^{-2} \text{ s}^{-1}$) k Conductivity (kW m K^{-1}) k_s Salt mass transfer coefficient (m s^{-1}) MW_w Water molecular weight (kg mol^{-1}) P^* Saturation pressure (Pa) P_{air} Pore air partial pressure (Pa) P_T Total pressure (Pa) Q Heat flow (kW) R Gas constant ($\text{kJ mol}^{-1} \text{ K}^{-1}$) T Temperature (K) x Salt mole fraction (mol mol^{-1}) δ Membrane thickness (m) ε Membrane porosity (%) ρ Density (kg m^{-3}) τ Membrane tortuosity (-)
	Membrane coefficient $C_m = \left[\frac{1}{\frac{2\pi \varepsilon d_p}{3} \tau \delta} + \frac{1}{\frac{\varepsilon MW_w P_T D}{\tau \delta R T_m P_{air}}} \right]^{-1}$	
	Solute concentration $x_{H,m} = x_H \cdot \exp\left(\frac{J}{\rho_H k_s}\right)$	
	Heat transfer	
	Hot side $Q_H = F_H \cdot C_p \cdot (T_{H,o} - T_{H,i})$ $Q_H = A \cdot h_H \cdot (T_H - T_{H,m})$	
Membrane $Q_m = A \left(\frac{k_m}{\delta} \cdot (T_{H,m} - T_{C,m}) + J \cdot \Delta H^{vap} \right)$		
Cold side $Q_C = F_C \cdot C_p \cdot (T_{C,o} - T_{C,i})$ $Q_C = A \cdot h_C \cdot (T_{C,o} - T_C)$		
Subscripts C Cold side H Hot side i In m Membrane o Out		

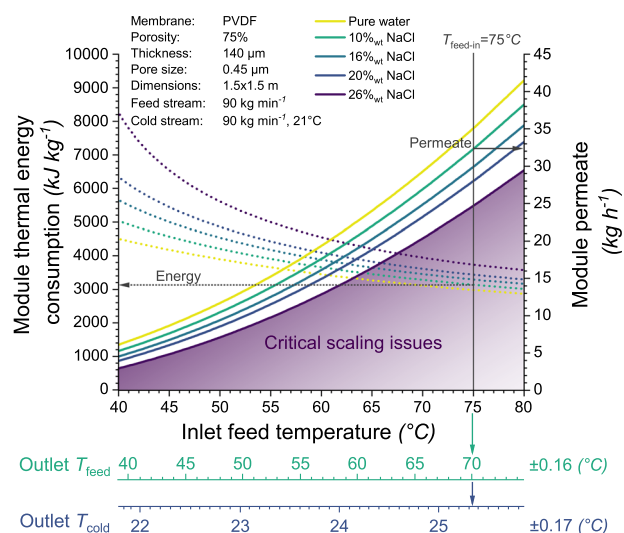


Fig. 6 Membrane distillation module performance curve. Example of a performance curve for a MD module constructed with a membrane with nominal parameters indicated in the legend. Given the input conditions of feed temperature (x -axis) and salinity, the module permeate rate is read to the left from the solid isoconcentration lines and the thermal energy consumption to the right of the dashed isoconcentration lines. The outlet streams' temperatures are obtained from the bottom axis of the chart. If the module is fed with a 10%_{wt} NaCl brine at 75 °C, the predicted outcomes from the curve are: a permeate rate of 32.3 kg h⁻¹, energy consumption of 3132 kJ kg⁻¹, and final hot and cold streams temperature of 70.1 and 25.3 °C, respectively.

modules' performances. STEC depends on the permeate rate and just indirectly on the membrane area; since the energy consumption depends only on the permeate productivity, which decreases for larger modules, the module sizing must consider the investment as well as maintenance expenses, over the operational costs.

From the MD module to the desalination process design

Once a membrane shows feasibility under certain operational conditions for a target MD process, process design must be carried out for techno-economic evaluations. In this context, two strategies or routes are identified (Fig. 4). First, the empirical route, where MD prototypes are built with arbitrary sizing criteria considering lab-scale results, and then tested. If the prototype does not reach the required performance, a new one has to be designed, built, and tested again, in a trial-and-error methodology. Although extensively used, this iterative process is a highly expensive strategy that not all research projects can afford. A second alternative is the so-called fundamental basis route. As discussed in the previous section, the module can be first designed using an MD model such as the one proposed for DCMD in this work. This allows for considering several scenarios, in which a range of design variables as well as equipment dimensions and geometries can be simulated, leading to considerable time and cost reduction. Process design based on fundamental theories can be incorporated into the empirical trial and error route to set a starting point, thus reducing expensive module manufacturing.

Furthermore, proportional scale-up designs are typically carried out in the empirical route, i.e., a proportional number of MD modules is arranged in consecutive stages to reach the target productivity. The final process performance is usually obtained from the empirical data of the tested module times the number of stages. Results from this approach are misleading since no variations in the interstage operational parameters are considered.

The increased deviation between both scale-up strategies as stage number (M) grows, can be seen in Fig. 5. Along the process, the treated salty water gets more concentrated, the so-called retentate or brine, and the permeability performance of the same module drops stage by stage. Additionally, more thermal energy is required to break interactions between the water and the salt ions, and consequently, the whole distillation process is undersized. Note that the STEC presented in this example does not consider the initial stream heating, energy recovery, or ambient losses. Certainly, such deviations from the real process have a significant effect on the operational and capital costs of techno-economic evaluations. Multi-stage DCMD analysis results are available in the Supplementary Information.

The MD module performance curve

In order to connect the MD phenomenological modeling and the scale-up steps, a thorough description of the optimized module must be provided. Herein, we proposed the "MD module performance curve" (Fig. 6), where the inlet feed-stream conditions, such as temperature and salinity, can be used to predict the module productivity, energy requirement, and outlet operational values. The curves in the graph have been built from data obtained with the developed phenomenological model and computational simulations, mimicking centrifugal pump curves, and summarize the DCMD equipment's expected behavior. The chart is made for a module of nominal properties (membrane material, morphology, and area, as well as flow rates and cold stream inlet temperature). It provides information about the permeate rate through the module (solid lines read to the left); the stage thermal energy consumption (dashed lines read to the right); and the streams outlet temperatures (read at the bottom axis), for which the feed salinity has no significant effect. Results have been previously validated with experimental data found in the literature^{48,49}. Validation data and results are available in Supplementary Information.

The proposed MD module performance curve allows for a better understanding of the water recovery process as well as a finer sensibility analysis within stages. It is possible to identify operational windows and accurately predict feasible conditions to work at. As seen in Fig. 6, the module performance is sensitive to feed conditions; as the feed salt concentration increases along the stages, the water permeation is reduced, and more energy is required. Thus, the upstream output affects the next stage input. Ignoring this effect with a proportional scale-up approach leads to erroneous technical-economic evaluations.

MD technology development perspectives

The evolution of emerging technologies can be represented by the hype cycle model⁵⁰, where a peak of inflated expectations at the beginning of the cycle is followed by disillusionment and enlightenment, before reaching a final stage of productivity. MD has been in the inflated expectations stage for a long time, and no major signs of enlightenment are evidenced, thus it is probably now in the disillusionment valley. Efforts to reach technological maturity must be put on the right track, avoiding missing opportunities and waste of resources in expensive iterative pilot assays. Although both routes, empirical trial and error and fundamental basis, lead to the same outcome, conceptual and basic engineering designs should come before detailed engineering. Therefore, a suitable strategy should start from the phenomenological descriptions, reinforcing the link with the real applications. We propose following the fundamental basis strategy under a coupled phenomenon model to aid in the implementation of MD at an industrial level. It is also imperative for laboratory-based researchers to measure and report the parameters and setups' geometries that determine the MD

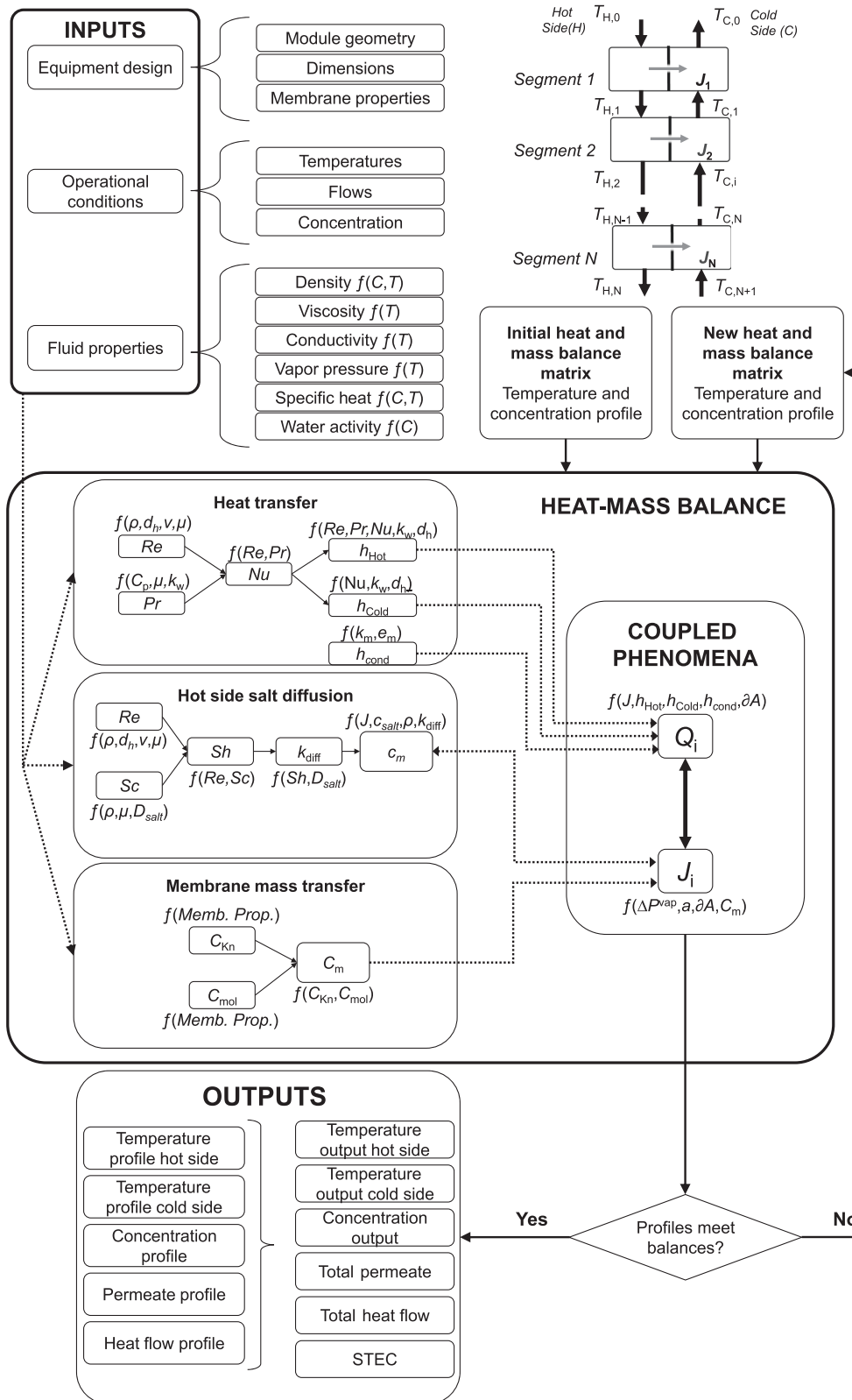


Fig. 7 DCMD module simulation algorithm developed in this work based on a coupled mass and heat transfer model. Re , Reynold number; ρ , density; d_h , hydraulic diameter; v , velocity; μ , viscosity; Pr , Prandtl number; C_p , heat capacity; k_w , water conductivity; Nu , Nusselt number; k_m , membrane conductivity; e_m , membrane thickness; h_{cond} , membrane heat transfer coefficient by conductive mechanism; h_{Hot} , hot side convective heat coefficient; h_{Cold} , cold side convective heat coefficient; Sc , Schmidt number; Sh , Sherwood Number; k_{diff} , salt mass transfer coefficient; D_{salt} , salt diffusion coefficient; c_m , concentration of salt in membrane surface; C_{Kn} , Knudsen diffusion coefficient; C_{mol} , molecular diffusion coefficient; C_m , membrane coefficient; A , membrane area; J_i , permeate flux; Q_i , transmembrane heat flow; ΔP^{vap} , vapor pressure difference between both sides of the membrane; a , water activity.

hydrodynamics. Additionally, mass and energy balances should be carried out to validate experimental results.

The approach we propose in this work helps to solve the issues of conventional proportional scale-up methods and allows for more accurate results. Plotting the MD module performance curves offers a simple yet comprehensive way to obtain operational MD module outcomes, which we believe will launch the MD technology in both academic and applied fields.

The need for overcoming the MD industrial developmental barriers was recognized almost two decades ago, pointing out the need to avoid redundant research on already-known topics⁵¹. Nevertheless, still exist several knowledge gaps where research efforts should focus on. Understanding the membrane wetting phenomena is key to assessing how the membrane material and its morphology affect vapor permeation and salt rejection. Yet, fundamental descriptions are not sensitive enough to be accurately implemented into the models. Likewise, membrane coefficient correlations, one of the key scaling parameters, need to be improved to be able to predict membrane performance. Lastly, custom energy integration methods, as well as pressure loss calculations, are required to complete the whole process design. Moreover, by adopting solar energy to provide hot and cold energy sources altogether, MD might reach greater thermodynamic efficiency than electricity-powered RO. The advancement in these topics together with the given insights in this work, will warrant the competitiveness of MD and ultimately will reach its technological maturity.

METHODS

Phenomenological modeling

A coupled mass and heat transfer approach was used to set up the DCMD model. A flat sheet configuration, such as that in plate and frame modules, was selected, where three parts were defined: hot side, membrane, and cold side. The brine was fed at a high temperature to the hot side channel, while a low-temperature water stream was fed in countercurrent to the cold side channel. The flow of volatile species permeating through the membrane, called permeate, was obtained through the equations displayed in Table 1. The driving force for mass transfer is the species' chemical potential gradient at both sides of the membrane that arises from the difference in the vapor pressures due to the temperature gradient. Several models have been proposed to describe the membrane coefficient being the couple Knudsen and molecular diffusion mechanisms as the common starting point. On the hot side, the diluted salts show a mass transfer from the bulk stream concentrating near the membrane surface thus affecting the effective vapor pressure. This effect is quantified by water activity.

An adiabatic module was assumed to describe the heat transfer mechanism. On the hot side, convective heat transfer towards the membrane surface from the bulk stream takes place. Across the solid phase of the membrane, conductive heat flow takes place towards the cold side, while within the free space of the pores, energy is carried by the volatile molecules quantified by the enthalpy of vaporization. Lastly, a convective mechanism takes place from the permeate surface of the membrane to the bulk of the fluid on the cold side.

Physicochemical properties correlations and thermodynamics compounds data are broadly available elsewhere.

DCMD numerical simulation

Due to the difficulty to obtain an analytical solution to the coupled phenomenological model, the MD modeling was carried out by computational iterative simulation. A custom script routine was programmed to perform process resolution. The simulation algorithm is lineout in Fig. 7. The membrane surface is divided into several interrelated sections in a "balance matrix" of

temperatures and salt concentration profiles⁵². The phenomenological model is independently applied to every sub-division. Given the process boundary conditions (streams initial temperatures, composition, and flowrates) and defining the DCMD module specifications (dimension and membrane characteristics), the algorithm aims to meet the mass and energy balances. To ensure the solution convergence, the modified Powell's method, available from open-source libraries, was implemented to iterate the matrix values until it met the balance of both global and every module sub-division.

DATA AVAILABILITY

The datasets derived from this work are available from the corresponding author upon reasonable request.

CODE AVAILABILITY

The simulation code has been deposited in the Zenodo digital repository (<https://doi.org/10.5281/zenodo.7212483>)⁵³.

Received: 23 June 2022; Accepted: 20 February 2023;

Published online: 03 March 2023

REFERENCES

- UN-Water. 2021: *Summary Progress Update 2021 – SDG 6 – water and sanitation for all*. Version: July 2021. Geneva, Switzerland https://www.unwater.org/sites/default/files/app/uploads/2021/12/SDG-6-Summary-Progress-Update-2021_Version-July-2021a.pdf (2021).
- Sood, A. & Smakhtin, V. Can desalination and clean energy combined help to alleviate global water scarcity? *JAWRA J. Am. Water Resour. Assoc.* **50**, 1111–1123 (2014).
- Glueckauf, E. Sea water desalination—in perspective. *Nature* **211**, 1227–1230 (1966).
- Alhaj, M., Hassan, A., Darwish, M. & Al-Ghamdi, S. G. A techno-economic review of solar-driven multi-effect distillation. *Desalin. Water Treat.* **90**, 86–98 (2017).
- Harandi, H. B., Rahnama, M., Jahanshahi Javaran, E. & Asadi, A. Performance optimization of a multi stage flash desalination unit with thermal vapor compression using genetic algorithm. *Appl. Therm. Eng.* **123**, 1106–1119 (2017).
- Shenvi, S. S., Isloor, A. M. & Ismail, A. F. A review on RO membrane technology: developments and challenges. *Desalination* **368**, 10–26 (2015).
- Mohammadifakhr, M., Grooth, J., de, Roesink, H. D. W. & Kemperman, A. J. B. Forward osmosis: a critical review. *Processes* **8**, 1–29 (2020).
- Jones, E., Qadir, M., van Vliet, M. T. H., Smakhtin, V. & Kang, S. The state of desalination and brine production: a global outlook. *Sci. Total Environ.* **657**, 1343–1356 (2019).
- Shahzad, M. W., Burhan, M., Ang, L. & Ng, K. C. Energy-water-environment nexus underpinning future desalination sustainability. *Desalination* **413**, 52–64 (2017).
- Curcio, E. & Drioli, E. Membrane distillation and related operations—a review. *Sep. Purif. Rev.* **34**, 35–86 (2005).
- Skuse, C., Gallego-Schmid, A., Azapagic, A. & Gorgojo, P. Can emerging membrane-based desalination technologies replace reverse osmosis? *Desalination* **500**, 114844 (2021).
- Abdel-Karim, A. et al. Membrane cleaning and pretreatments in membrane distillation—a review. *Chem. Eng. J.* **422**, 129696 (2021).
- Miladi, R., Frikha, N., Kheiri, A. & Gabsi, S. Energetic performance analysis of seawater desalination with a solar membrane distillation. *Energy Convers. Manag.* **185**, 143–154 (2019).
- Zaragoza, G., Andrés-Mañas, J. A. & Ruiz-Aguirre, A. Commercial scale membrane distillation for solar desalination. *npj Clean. Water* **1**, 20 (2018).
- Mohammadi Shamlou, E., Vidic, R. & Khanna, V. Optimization-based modeling and economic comparison of membrane distillation configurations for application in shale gas produced water treatment. *Desalination* **526**, 115513 (2022).
- Cerveira, G. S., de Magalhães, J. L. & de S. Antunes, A. M. Trends in membrane distillation for wastewater treatment. *J. Environ. Prot.* **12**, 106–124 (2021).
- Kiss, A. A. & Kattan Readi, O. M. An industrial perspective on membrane distillation processes. *J. Chem. Technol. Biotechnol.* **93**, 2047–2055 (2018).
- Conrow, E. H. Estimating technology readiness level coefficients. *J. Spacecr. Rockets* **48**, 146–152 (2011).

19. Adler, S., Beaver, E., Bryan, P., Robinson, S. & Watson, J. Vis. 2020: 2000 Sep. Roadmap <https://doi.org/10.2172/1218701> (2000).
20. Leaper, S., Abdel-Karim, A. & Gorgojo, P. The use of carbon nanomaterials in membrane distillation membranes: a review. *Front. Chem. Sci. Eng.* **15**, 755–774 (2021).
21. Boretti, A. et al. Outlook for graphene-based desalination membranes. *npj Clean. Water* **1**, 5 (2018).
22. Alkhatib, A., Ayari, M. A. & Hawari, A. H. Fouling mitigation strategies for different foulants in membrane distillation. *Chem. Eng. Process. - Process. Intensif.* **167**, 108517 (2021).
23. Wang, W. et al. Trade-off in membrane distillation with monolithic omniphobic membranes. *Nat. Commun.* **10**, 3220 (2019).
24. Liu, G. L., Zhu, C., Cheung, C. S. & Leung, C. W. Theoretical and experimental studies on air gap membrane distillation. *Heat. Mass Transf.* **34**, 329–335 (1998).
25. Leaper, S., Abdel-Karim, A., Gad-Allah, T. A. & Gorgojo, P. Air-gap membrane distillation as a one-step process for textile wastewater treatment. *Chem. Eng. J.* **360**, 1330–1340 (2019).
26. Olatunji, S. O. & Camacho, L. M. Heat and mass transport in modeling membrane distillation configurations: a review. *Front. Energy Res.* **6**, 1–18 (2018).
27. Hussain, A., Janson, A., Matar, J. M. & Adham, S. Membrane distillation: recent technological developments and advancements in membrane materials. *Emergent Mater.* **5**, 347–367 (2022).
28. Zahler, C. SolarSpring closes sales contract for an MD pilot system to be used in industrial water recycling project. *Press Release*. <https://storage.mfn.se/61c1936b-7466-46ed-bc42-f5899a531bdc/solarspring-closes-sales-contract-for-an-md-pilot-system-to-be-used-in-industrial-water-recycling-project.pdf> (2022).
29. Clean Industry Solutions Holding Europe AB. SolarSpring receives order to investigate treatment of process water from 'Dead Sea Works'. *Press Release*. <https://news.cision.com/clean-industry-solutions-holding-europe/r/solarspring-receives-order-to-investigate-treatment-of-process-water-from-dead-sea-works-c3548423> (2021).
30. Park, J. & Lee, S. Desalination technology in South Korea: a comprehensive review of technology trends and future outlook. *Membranes* **12**, 204 (2022).
31. Ashoor, B. Bin, Giwa, A. & Hasan, S. W. *Current Trends and Future Developments on (Bio-) Membranes: Membrane Desalination Systems: The Next Generation* (Elsevier Inc., 2018).
32. Guillen-Burrieza, E., Ruiz-Aguirre, A., Zaragoza, G. & Arafat, H. A. Membrane fouling and cleaning in long term plant-scale membrane distillation operations. *J. Memb. Sci.* **468**, 360–372 (2014).
33. Tuteja, A., Choi, W., Mabry, J. M., McKinley, G. H. & Cohen, R. E. Robust omniphobic surfaces. *Proc. Natl Acad. Sci. USA* **105**, 18200–18205 (2008).
34. Lee, J., Boo, C., Ryu, W. H., Taylor, A. D. & Elimelech, M. Development of omniphobic desalination membranes using a charged electrospun nanofiber scaffold. *ACS Appl. Mater. Interfaces* **8**, 11154–11161 (2016).
35. Horseman, T., Su, C., Christie, K. S. S. & Lin, S. Highly effective scaling mitigation in membrane distillation using a superhydrophobic membrane with gas purging. *Environ. Sci. Technol. Lett.* **6**, 423–429 (2019).
36. Huang, Y. X., Wang, Z., Jin, J. & Lin, S. Novel Janus membrane for membrane distillation with simultaneous fouling and wetting resistance. *Environ. Sci. Technol.* **51**, 13304–13310 (2017).
37. Lee, J. G., Kim, W. S., Choi, J. S., Ghaffour, N. & Kim, Y. D. A novel multi-stage direct contact membrane distillation module: design, experimental and theoretical approaches. *Water Res.* **107**, 47–56 (2016).
38. Lee, J. G. et al. Total water production capacity inversion phenomenon in multi-stage direct contact membrane distillation: a theoretical study. *J. Membr. Sci.* **544**, 126–134 (2017).
39. Francis, L., Ahmed, F. E. & Hilal, N. Advances in membrane distillation module configurations. *Membranes* **12**, 81 (2022).
40. Francis, L., Ghaffour, N., Alsaadi, A. S., Nunes, S. P. & Amy, G. L. Performance evaluation of the DCMD desalination process under bench scale and large scale module operating conditions. *J. Membr. Sci.* **455**, 103–112 (2014).
41. Amaya-Vías, D. & López-Ramírez, J. A. Techno-economic assessment of air and water gap membrane distillation for seawater desalination under different heat source scenarios. *Water* **11**, 2117 (2019).
42. Naidu, G., Tijing, L., Johir, M. A. H., Shon, H. & Vigneswaran, S. Hybrid membrane distillation: resource, nutrient and energy recovery. *J. Memb. Sci.* **599**, 117832 (2020).
43. Ghaffour, N., Soukane, S., Lee, J. G., Kim, Y. & Alpatova, A. Membrane distillation hybrids for water production and energy efficiency enhancement: a critical review. *Appl. Energy* **254**, 113698 (2019).
44. Shahzad, M. W., Burhan, M. & Ng, K. C. A standard primary energy approach for comparing desalination processes. *npj Clean. Water* **2**, 1 (2019).
45. Zaidi, S. J. & Saleem, H. *Reverse Osmosis Systems. Design, Optimization, and Troubleshooting Guide* (Elsevier, 2021).
46. Alkhdhiri, A., Darwish, N. & Hilal, N. Membrane distillation: a comprehensive review. *Desalination* **287**, 2–18 (2012).
47. Khayet, M. Membranes and theoretical modeling of membrane distillation: a review. *Adv. Colloid Interface Sci.* **164**, 56–88 (2011).
48. Schofield, R. W., Fane, A. G., Fell, C. J. D. & Macoun, R. Factors affecting flux in membrane distillation. *Desalination* **77**, 279–294 (1990).
49. Choi, J., Choi, Y., Lee, J., Kim, Y. & Lee, S. Exergy analysis of a direct contact membrane distillation (DCMD) system based on computational fluid dynamics (CFD). *Membrane* **11**, 525 (2021).
50. Dedehayir, O. & Steinert, M. The hype cycle model: a review and future directions. *Technol. Forecast. Soc. Change* **108**, 28–41 (2016).
51. El-Bourawi, M. S., Ding, Z., Ma, R. & Khayet, M. A framework for better understanding membrane distillation separation process. *J. Membr. Sci.* **285**, 4–29 (2006).
52. Lu, K.-J. & Chung, T.-S. *Membrane Distillation: Membranes, Hybrid Systems, and Pilots Studies* (CRC Press, 2020).
53. Ramos-Paredes, S. Towards the Technological Maturity of Membrane Distillation: the MD Module Performance Curve - Associated Code. <https://doi.org/10.5281/zenodo.7212483> (2022).

ACKNOWLEDGEMENTS

The authors acknowledge the Engineering and Physical Sciences Research Council (EPSRC) grant EP/S032258/1 for supporting this work. P. Gorgojo acknowledges Grant RYC2019-027060-I funded by MICIN/AEI/10.13039/501100011033 and by "ESF Investing in your future".

AUTHOR CONTRIBUTIONS

P.L.-P. draft writing and editing, methodology development, formal analysis and discussion, and state-of-the-art research; S.R.-P. modeling research, numerical simulation, formal analysis and discussion, and result validation; P.N. project conceptualization, outcomes discussion, manuscript revision, and supervision; P.G. outcomes discussion, manuscript revision, and supervision. P.L.-P. and S.R.-P. contributed equally as co-first authors.

COMPETING INTERESTS

The authors declare no competing interests.

ADDITIONAL INFORMATION

Supplementary information The online version contains supplementary material available at <https://doi.org/10.1038/s41545-023-00234-0>.

Correspondence and requests for materials should be addressed to Patricia Gorgojo.

Reprints and permission information is available at <http://www.nature.com/reprints>

Publisher's note Springer Nature remains neutral with regard to jurisdictional claims in published maps and institutional affiliations.



Open Access This article is licensed under a Creative Commons Attribution 4.0 International License, which permits use, sharing, adaptation, distribution and reproduction in any medium or format, as long as you give appropriate credit to the original author(s) and the source, provide a link to the Creative Commons license, and indicate if changes were made. The images or other third party material in this article are included in the article's Creative Commons license, unless indicated otherwise in a credit line to the material. If material is not included in the article's Creative Commons license and your intended use is not permitted by statutory regulation or exceeds the permitted use, you will need to obtain permission directly from the copyright holder. To view a copy of this license, visit <http://creativecommons.org/licenses/by/4.0/>.

© The Author(s) 2023